GEOMORPHOLOGICAL CHANGE DETECTION USING OBJECT-BASED FEATURE EXTRACTION FROM MULTI-TEMPORAL LIDAR DATA

A. C. Seijmonsbergen [a, *], N.S. Anders[a], W. Bouten[a]

[a] IBED, Institute for Biodiversity and Ecosystem Dynamics, Science Park 904, Amsterdam, The Netherlands - (a.c.seijmonsbergen, n.s.anders, w.bouten)@uva.nl

KEY WORDS: Geomorphology, LIDAR, Multi-temporal, Change Detection, Classification, Segmentation

ABSTRACT:

Multi-temporal LiDAR DTMs are used for the development and testing of a method for geomorphological change analysis in western Austria. Our test area is located on a mountain slope in the Gargellen Valley in western Austria. Six geomorphological features were mapped by using stratified Object-Based Image Analysis (OBIA) and segmentation optimization using 1m LiDAR DTMs of 2002 and 2005. Based on the 2002 data, the scale parameter for each geomorphological feature was optimized by comparing manually digitized training samples with automatically recognized image objects. Classification rule sets were developed to extract the feature types of interest. The segmentation and classification settings were then applied to both LiDAR DTMs which allowed the detection of geomorphological change between 2002 and 2005. FROM-TO changes of geomorphological categories were calculated and linked to volumetric changes which were derived from the subtracted DTMs. Enlargement of mass movement areas at the cost of glacial eroded bedrock was detected, although most changes occurred within mass movement categories and channel incisions, as the result of material removal and/or deposition. The proposed method seems applicable for geomorphological change detection in mountain areas. In order to improve change detection results, processing errors and noise that negatively influence the segmentation accuracy need to be reduced. Despite these concerns, we conclude that stratified OBIA applied to multi-temporal LiDAR datasets is a promising tool for of geomorphological change detection.

1. INTRODUCTION

1.1 Motivation and objectives

Geomorphological mapping is a well-recognized technique to document landforms, materials, morphometry and genesis of landforms. It is used in landscape reconstructions, as additional data to understand climate proxies and is used in applied studies such as hazard and risk assessment and landscape conservation. Classical geomorphological maps are hand drawn paper maps, mostly prepared by an expert using a package of point, line and area symbols, which are combined to display geomorphological features. For an overview of such mapping systems is referred to Seijmonsbergen et al. (2011). The wide availability of DTMs and the integration of both geographical information systems (GIS) and remote sensing (RS) technology have changed the routines of modern geomorphological map production. Computer-generated geomorphological mapping uses DTMs, ortho-rectified imagery, and (semi-) automated routines for feature extraction and landform mapping in a digital environment and reduces field visits. Digital applications of modern geomorphological information layers are being developed and are made available more easily to end-users, e.g. via web-based portals.

The field of "geomorphometry"- the science of quantitative land-surface analysis (Hengl and Reuter, 2008) - is concerned with the automated extraction of geomorphological features from DTMs by using Land Surface Parameters (LSPs) and statistical analyses. Next to this development, Object-Based Image Analysis (OBIA) is widely used for landform classification (Drăguţ and Blaschke 2006) and other geomorphological applications by using complex workflows for the segmentation and classification of both high-resolution imagery and/or DTMs (Blaschke 2010).Automated techniques of feature extraction and geomorphological mapping allow objective and systematic analysis of digital elevation data, which paves the way for quantitative comparison of multi-temporal data to model detailed and specific topographic change over time.

Our objective is to test stratified object-based segmentation and classification on a multi-temporal 1m resolution LiDAR dataset and to prepare and evaluate a geomorphological change detection layer in a mountainous area suffering from slope instability processes.

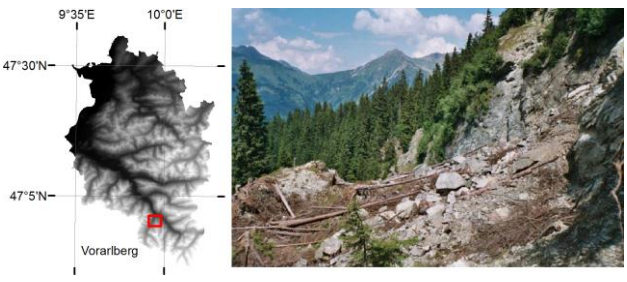

Figure 1. The study area (red box, left) is located in Vorarlberg, the westernmost state of Austria. Characteristic to the area are surface mass movements in metamorphic bedrock.

1.2 Overview

There are currently three important trends in modern geomorphological mapping (Seijmonsbergen et. al (2011):

* Corresponding author

1. Digitizing existing classical geomorphological maps into GIS databases 2. Updating classical digitized geomorphological maps by adding detailed information which has been manually or automatically extracted from high resolution DTMs and 3. Automated and semi-automated geomorphological mapping using DTM-derived LSPs, OBIA and rule sets development.

The use of LiDAR technology has accelerated the development of analysis tools and work flows for use in the automated approach, especially in mountains, where accessibility is difficult and detailed maps are often scarce. Feature extraction using LSPs and/or object-based classification has been tested and applied in a number of mass movement studies (e.g. McKean and Roering 2004; Glenn et al. 2006). Traditionally, mass movement change detection was studied by detecting changes in multi-spectral temporal satellite image and air-photo analyses. Nowadays, OBIA is increasingly applied on DTMs (Anders et al, 2011a), and initiatives for preparation of feature signature libraries (Anders et al., 2011b) or combining spectral and DEM derived signatures (e.g. Stumpf and Kerle 2011, Aksoy and Ercanoglu 2012) have been undertaken to map landscape as a whole (MacMillan et al. 2000; Van Asselen and Seijmonsbergen 2006; Anders et al. 2011b).

1.3 Study area

We have selected part of a hillslope in the Gargellen Valley, in the State of Vorarlberg, western Austrian Alps (Figure 1) because multi-temporal LiDAR datasets were available, and the landslide and fluvial activity is high, guaranteeing that change over this time interval is expected. The area is part of the crystalline Silvretta nappe and is underlain by formations composed of ortho- and paraschists, amphibolites and micaschists. This crystalline nappe was dragged over East Alpine sedimentary series during alpine orogenesis which resulted in severe tectonic deformation and weakening of rock strength. In addition, intense and repeated glacial erosion during the Pleistocene has resulted in steepening of slopes. This has triggered tensional rebound, which accelerated a variety of geomorphological processes such as rock slides, rock fall and fluvial erosion, carving deeply into the disintegrated and weathered bedrock (Van Noord et al., 1996).

2. METHODS

2.1 Data and software

Two LiDAR data sets from a December 2002 and a November 2005 flight were used. The raw point data were acquired, filtered and interpolated into 1m resolution LiDAR raster DEMs by TopScan (http://www.topscan.de/). We had access to a Canopy Height Model (CHM) and the DTMs of both years. Six coverages of digital multi-temporal ortho-rectified panchromatic, color and infrared air-photos, with resolutions between 12.5cm and 100cm were available from the mid nineteen-fifties to 2010.The segmentation and classification was performed in eCognition Developer8.7, the segmentation accuracy assessments and optimization were carried out in Python+GDAL/OGR, while change detection calculations and map visualizations were performed in ArcGIS10.

2.2 Processing

A workflow visualizing the individual main processing steps are displayed in Figure 2. These steps follow and elaborate on the approach of Anders et al., (2011a). Their analysis is divided into four steps: 1. data preparation, 2. parameterization, 3. stratified feature extraction using OBIA and 4. validation. As a further step 5 we introduce the calculation of a geomorphological change detection layer. Included in this additional step 5 is the volumetric change between the two DTMs, linked to the geomorphological categories that occur in the area.

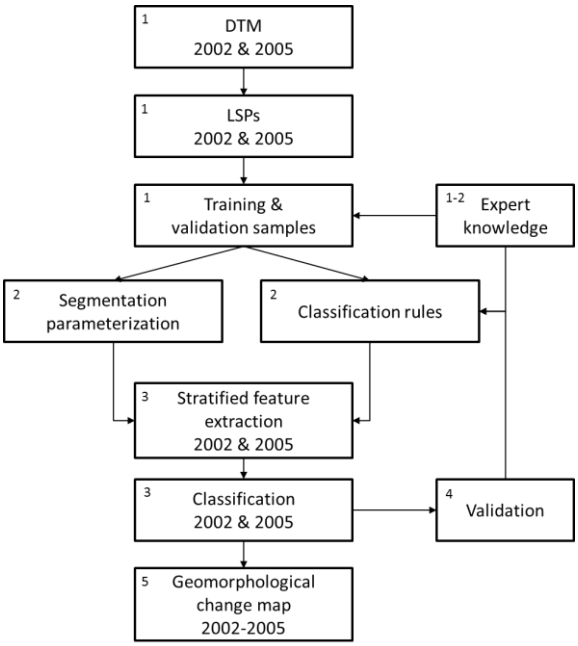

Figure 2. General workflow of the method. The numbers in the boxes correspond to the processing steps in the text.

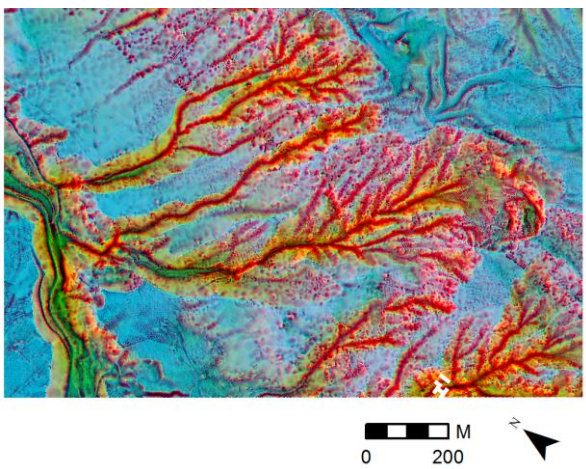

Figure 3. RGB false color LSP composite layer combination of slope angle, openness25m and openness 250m.

Six contrasting geomorphological feature classes were recognized and incorporated: 1. fluvial incision, 2. glacially eroded bedrock, 3. alluvial/debris fans, 4. shallow mass movements, 5. flow/slide deposits and 6. deep-seated mass movements. The step by step procedure comprises:

1. Data preparation. This step comprises the calculation of LSPs from the two LiDAR DTMs, namely a slope angle layer, an elevation percentile layer (EPC) and two topographic openness layers, with a kernel size of 25x25m (TO25) and 250x250m (TO250) (Yokayama et al., 2002). For the

classification of fluvial incisions, an upstream area layer was constructed by using the D8 method as implemented in ArcGIS (Jenson and Domingue, 1988).

A Red-Green-Blue (RGB) false color LSP composite layer was produced by combining the slope angle, TO25 and TO250 layers (Figure 3). Such false color LSP composites are independent of artificial illumination, like hill shade maps are. RGB layers do not suffer from disguise of boundaries by shadows or clouds on air-photos, and thus allow precise landform delineation, either manually or through automatic segmentation. The RGB layer was used to create a) training samples for each category to determine optimal scale parameters for the segmentation of the two DTMs, and b) a validation set of manually delineated landforms to test the performance of the resulting classification.

2. Parameterization. Image objects were derived from segmentations with scale parameters ranging from 1-1000. The sets of objects were compared with the training samples of each geomorphological feature type by calculating 2D frequency distribution matrices (using the slope and TO250 LSPs). The sum of absolute error between the matrices of training samples and eCognition objects were used as a measure of segmentation error. The scale parameter related to the smallest segmentation error was considered most accurate for segmenting the specific geomorphological feature. For in-depth information regarding the parameter optimization we refer to Anders et al. (2011a).

3. Stratified feature extraction. In this step, feature-specific segmentation and classification rules are applied and the six categories are extracted separately in a stratified way: smaller and distinct features first, followed by extraction of larger features.

4. Validation. Qualitative comparison and validation of the classified geomorphological feature types were carried out by manual comparison to the existing 1:10.000 scale classical geomorphological map sheet St.Gallenkirch (Van Noord, 1996). In addition, six temporal ortho-photo series were inspected to validate the resulting change maps.

A quantitative validation of classification results was performed based on the method described by Congalton and Green (1999). Both the classification and the validation samples of step 1 were rasterized into 5x5m grid cells. Then the labels of classified grid cells and the validation grid cells were compared and summarized into a confusion matrix. The user's, producer's and overall accuracies were determined for the six feature classes to quantify the performance of the classifications.

5. Change detection. A geomorphological change layer was prepared by listing the change per geomorphological feature type as FROM-TO changes. These were attributed with volumetric change information by subtracting the 2005 from the 2002 DEM and using an overlay operation with the geomorphological change layer.

The method requires mimimum expert-knowledge input, which was obtained from a short field visit and by consulting the multi-temporal ortho-photos, which were draped over the LiDAR DTM and CHM, allowing detailed genetic interpretation of landform and evaluation of locations of potential change.

3. PRELIMINARY RESULTS

3.1 Segmentation parameterization

Figure 4 shows the calculated error against the scale parameter value for the six feature types. The optimal SP varies between 35 (fluvial incision) and 150 (shallow mass movement). The error values indicate that alluvial/debris fan (error 0.39) has been more accurately segmented than deep seated mass movement (error 0.57). The surface morphology of the debris fan is clearly "smoother" or more "homogeneous" than that of the deep seated mass movements occurring in the area, which may also inherit "signature" characteristics of former feature types such as glacially eroded bedrock.

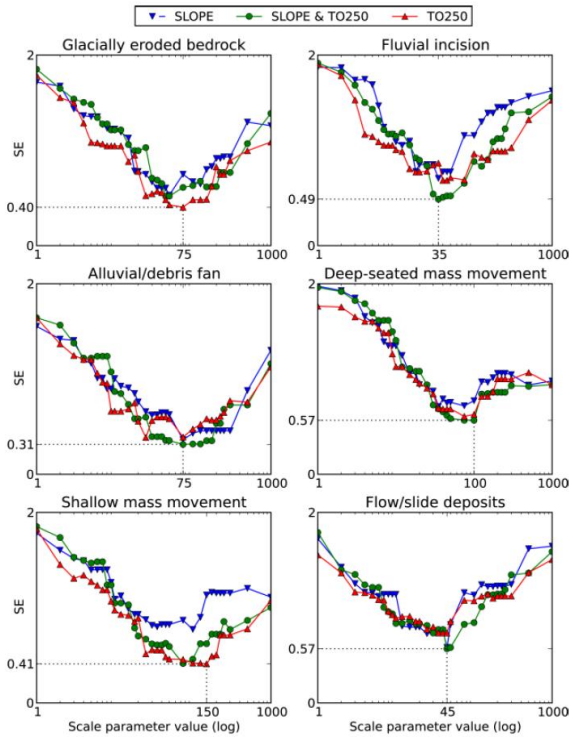

Figure 4. Segmentation Error (SE) plotted against the scale parameter value for each geomorphological feature. The three colors in the graphs refer to segmentation results calculated with the LSPs 'slope', 'slope and TO250 and TO250.

	Glacially eroded bedrock	Fluvial incision	Alluvial/debris fan	Deep mass m.	Shallow mass m.	Flow/slide dep.
Segmentation						
Scale parameter	75	35	75	100	150	45
LSPs	TO250	Slope, TO250	Slope, TO250	TO250	Slope, TO250	Slope, TO250
Classification						
Mean EPC [%]	> 55		> 45			
Mean TO250 [°]	> 160	< 160	> 160			130-170
Mean slope [°]		> 20	< 25		> 30	< 45
Std DTM [-]		< 4		> 8		
Std slope [-]					> 5	
Dist. to river [m]		< 50				

Table 1. Segmentation and classification settings used in the classification of both LiDAR DTMs.

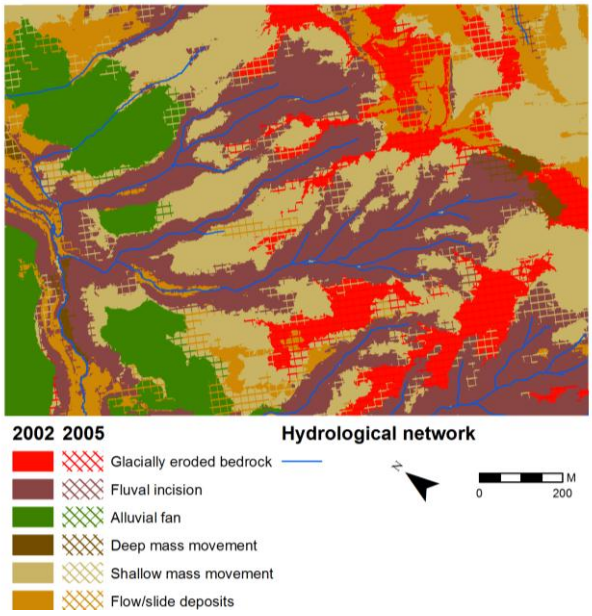

Figure 5. Classifications for 2002 (full color) overlain with the changes of the 2005 classification (hatched).

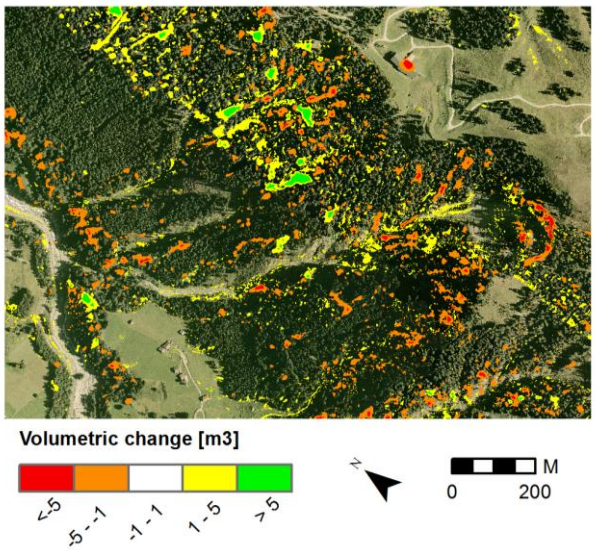

Figure 6. Volumetric change in m^3. The backdrop image is an ortho-photo of 2006.

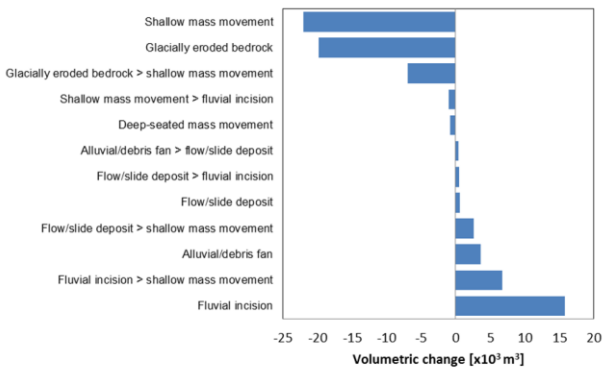

Figure 7. Volumetric changes (removal and deposition) per geomorphological feature class and the most important "FROM-TO" changes.

3.2 Classification

The parameters and criteria used in the classification of the two LiDAR DTMs are listed for each geomorphological feature type in table 1. The order of stratified classification that produced the best result was 1) fluvial incision, 2) alluvial fan/debris fans, 3) glacially eroded bedrock, 4) deep-seated mass movement, 5) shallow mass movement, 6) flow/slide deposits. The geomorphological maps generated for the two dates are displayed in Figure 5. Although segmentation is thought to be influenced by noise in the two DTMs, the overall patterns correlate well. Based on these multi-temporal geomorphological maps and DTMs, the change analysis has been made.

3.3 Change analysis

In Figure 5 the classifications of 2002 and 2005 are displayed. The classification of 2005 has been indicated by a hatching. In this way the locations where the 2005 classification is equal to the 2002 classification the hatching will overlap the original color and no difference or change is visible. On the other hand, change between different classes is clearly visualized.

Figure 6 presents the volumetric change (in m^3) between 2002 and 2005, by taking into account a threshold value of -1 to +1m (regarded as no change). The map is underlain by a subset of the 25cm resolution true color ortho-photo of 2006.

In Figure 7 the most evident volumetric and „FROM-TO" changes per geomorphological feature class are presented as negative and positive change. Positive change (deposition) predominantly occurred predominantly within fluvial incisions and on alluvial/debris fans. Positive volumetric change also occurred where fluvial incisions changed into slopes with shallow mass movement. Negative change (removal of material) occurred predominantly within slopes affected by shallow mass movement and glacially eroded bedrock. Slopes with deep seated mass movement were only slightly altered by removal of material. It appears that some unlikely transformations occurred for the unit shallow mass movement, which erroneously changed into glacially eroded bedrock.

Negative values correlate to numerous small bank failures that occurred along the slopes of fluvial incisions or along the steeper backs carps located on the upper steep slopes. Most positive changes reflect sediment, derived these upper landslide areas, which has transported and deposited near a distinct break in slope, occurring in most channels halfway to the main Suggadin River valley floor, and which probably occurred after heavy rainfall in August 2005 (Chiari et al., 2008). The banks of the Suggadin River also show a denser pattern of negative values, which is attributed to bank retreat, initiated by local landslides and lateral bank erosion.

3.4 Accuracy assessment

In Table 2 the accuracy assessment is presented in a confusion matrix (Congalton and Green, 1999). The overall classification accuracy was 84% for 2002 and 87% for 2005. Review of the user's and producer's accuracy shows that a grouping of three well classified feature types appears in both datasets (glacially eroded bedrock, alluvial fan/debris fan and shallow mass movement), that two feature types (deep mass movement and fluvial incision) are moderately well classified, and that the classification of the flow/slide deposits results in a poor classification. This could relate to overlapping topographic

properties or signatures between geomorphological features, the few validation pixels used in the accuracy assessment or the order of stratified classification followed.

			Validation samples						
		Year	Glacially eroded bedrock	Fluvial incision	Alluvial/debris fan	Deep mass m.	Shallow mass m.	Flow/slide dep.	Total
Classification	Glacially eroded bedrock	2002	**264**	0	0	93	17	0	374
		2005	**331**	0	0	102	21	0	454
	Fluvial incision	2002	0	**103**	0	45	4	70	222
		2005	0	**75**	0	59	0	54	188
	Alluvial/debris fan	2002	0	0	**886**	0	0	0	886
		2005	0	0	**903**	0	0	0	903
	Deep mass m.	2002	0	0	0	**243**	0	4	247
		2005	0	0	0	**224**	0	6	230
	Shallow mass m.	2002	54	0	0	25	**404**	0	483
		2005	7	0	0	25	**404**	8	444
	Flow/slide dep.	2002	28	0	17	6	0	**12**	63
		2005	8	0	0	2	0	**8**	18
	Total	2002	346	103	903	412	425	86	2275
		2005	346	75	903	412	425	76	2237
	User's accuracy	2002	71	46	100	98	84	19	
		2005	73	40	100	97	91	44	
	Producer's accuracy	2002	76	100	98	59	95	14	
		2005	96	100	100	54	95	11	
	Overall accuracy	2002	84						
		2005	87						

Table 2. Comparison between the classification results and validation sample data for the six feature classes.

4. CONCLUSIONS

Current geomorphological change detection methods mainly focus on subtraction of multi-temporal DTMs, and change interpretation afterwards. Our OBIA approach includes „From-To" changes as well as volumetric changes per geomorphological category, as the result of multi-temporal semi-automated classifications for different years, using a stratified classification approach.

The preliminary results and the experience obtained in working with multi-temporal DTMs leads to the following conclusions: The geomorphological change detection method gives insight in both the spatial changes and in volumetric changes that occurred in the landscape, which shows added value over existing geomorphological change detection methods (DeWitte et al., 2008).

In areas where volumetric changes occurred we expected the DTM derived LSP signals to have changed likewise, forcing categorization in a different landform class. This seems true for the mass movement feature classes that enlarge at the cost of non-mass movement units. In case volumetric changes occur within the same feature classes, the segmentation signals and classification rules remain the same, indicating that such categories may deepen or become covered, without being "detected" as different in the signal. It was observed that this is strongly related to fluvial incisions.

The noise present in the processed LiDAR DTMs does influence the final change product. This noise can be reduced during processing of the LiDAR, preferentially by using similar reflection densities and comparable interpolation techniques. We strongly suspect that the differences in vertical accuracy between the two DTMs are largest in forested and steep terrain, as a consequence of amongst others point density variation. For now, we used a threshold value to cope with these supposed uncertainties and errors.

The proposed method is based on transferable segmentation parameters and classification rule sets and needs minimum expert-knowledge input. We see great monitoring potential application in hazard and risk studies, rate of change analyses, and scale dependant research (Hay et al. 2003) and vulnerability assessments with increasing availability of new multi-temporal LiDAR data.

5. ACKNOWLEDGEMENTS

This research is financially supported by the Virtual Lab for e-Science (vl-e) project. We are grateful to the "Land Vorarlberg" (www.vorarlberg.at) in Austria for free use of the LiDAR data. We used the GIS and remote sensing facilities provided by the GIS-studio of IBED, www.GIS-studio.nl.

REFERENCES

Aksoy, B., Ercanoglu, M., 2012. Landslide identification and classification by object-based image analysis and fuzzy logic: An example from the Azdavay region (Kastamonu, Turkey) *Computers & Geosciences* 38, pp. 87-98.

Anders, N.S., Seijmonsbergen, A.C., Bouten, W., 2011a. Segmentation optimization and stratified object-based analysis for semi-automated geomorphological mapping, *Remote Sensing of Environment*, 115, pp. 2976-2985.

Anders, N., Smith, M., Seijmonsbergen, Bouten, W. 2011b. Optimizing object-based image analysis for semi-automated geomorphological mapping. In T. Hengl,. Evans, I.S., Wilson J.P., Gould, M. (Eds.), *Proceedings of Geomorphometry 2011*, pp. 117-120.

Blaschke T., 2010. Object-based image analysis for remote sensing. *ISPRS journal of Photogrammetry and Remote Sensing* 65(1), pp. 2-16.

Chiari, M., Mair, E. Rickenmann, D., 2008. Modelling sediment stream and comparison of the morphologic change with lidar data. *Interpraevent Conference Proceedings*, band I pp. 295 – 306

Congalton, R., Green, K., 1999. "Assessing the accuracy of remotely sensed data: principles and practices". Lewis Publishers, Boca Raton.

Dewitte, O., Jaselette, J.-C., Cornet, Y., Van den Eeckhout, M., Collignon, A., Poesen, J., Demoulin, A., 2008. Tracking landslide displacements by multi-temporal DTMs: A combined aerial stereophotogrammetric and LIDAR approach in western Belgium. *Engineering Geology*, 99, pp. 11-22.

Drăguţ, L., Blaschke, T., 2006. Automated classification of landform elements using object-based image analysis. *Geomorphology*, 81, pp. 330–344.

Glenn, N. F., Streutker, D. R., Chadwick, D. J., Thackray, G. D., Dorsch, S. J., 2006. Analysis of lidar-derived topographic information for characterizing and differentiating landslide morphology and activity. *Geomorphology*, 73, pp. 131–148.

Hay, H.J., Blaschke, T., Marceau, D.J., Bouchard, A., 2003. A comparison of three methods for the multiscale analysis of landscape structure. *ISPRS Journal of Photogrammetry and Remote Sensing*, 57, pp. 327-345.

Hengl, T., Reuter, H., (Eds.). 2008. *Geomorphometry: Concepts, software, applications.* Elsevier, Amsterdam, 765 pp.

Jenson, S. K., J. Domingue. J.O., 1988. Extracting Topographic Structure from Digital Elevation Data for Geographic Information System Analysis. *Photogrammetric Engineering and Remote Sensing* 54, pp. 1593-1600.

MacMillan, R.A., Pettapiece, W.W., Nolan, S.C., Goddard, T.W., 2000. A generic procedure for automatically segmenting landforms into landform elements using DEMs, heuristic rules and fuzzy logic. *Fuzzy Sets and Systems*, 113, pp. 81–109.

McKean, J., Roering, J., 2004. Objective landslide detection and surface morphology mapping using high-resolution airborne laser altimetry. *Geomorphology*, 57, pp. 331–351.Seijmonsbergen, A. C., Hengl, T., & Anders, N. S. (2011). Semi-automated identification and extraction of geomorphological features using digital elevation data. In M. Smith, P. Paron, & J. Griffiths (Eds.), *Geomorphological Mapping: Methods and Applications* Vol. 15 of Developments in Earth Surface Processes Elsevier, Amsterdam, pp. 297-335.

Stumpf, A., Kerle, N., 2011. Object-oriented mapping of landslides using Random Forests. *Remote Sensing of Environment*, 115(10), pp. 2564-2577

Van Asselen, S., Seijmonsbergen, A.C., 2006. Expert-driven semi-automated geomorphological mapping using a laser DTM. *Geomorphology*, 78(3-4), pp. 309-320.

Van Noord, H., Rupke, J., Seijmonsbergen, A.C., de Graaff, L.W.S., 1996. Integralpilotstudie Montafon: geomorphological-geotechnical and natural hazard maps at scale 1:10.000 in the eastern Rätikon Mountains and the Montafon region, Vorarlberg. Report to the Bundesministerium für Land- und Forstwirtschaft, 71 pp.

Yokoyama R, Shirasawa M., Pike R.J., 2002. Visualizing topography by openness: a new application of image processing to digital elevation models. *Photogrammetric engineering and remote sensing*, 68, pp. 257-265.